Title: **Presynaptic A$_{2A}$ adenosine receptors dampen CB$_1$ cannabinoid receptor-mediated inhibition of corticostriatal glutamatergic transmission**

Running Title: **A$_{2A}$R-CB$_1$R interaction in corticostriatal terminals**

S G Ferreira[1-3,5], F Q Gonçalves[1], J M Marques[1], Â R Tomé[1], R J Rodrigues[1], I Nunes-Correia[4], C Ledent[7], T Harkany[8,9], L Venance[10], R A Cunha[1,5], and A Köfalvi[2,6]

[1]*Neuromodulation Group,* [2]*Laboratory of Neuromodulation and Metabolism,* [3]*Doctoral Programme in Experimental Biology and Biomedicine, and* [4]*Flow Cytometry Unit, CNC-Center for Neuroscience and Cell Biology, and* [5]*Faculty of Medicine, and* [6]*Institute for Interdisciplinary Research, University of Coimbra, 3004-504 Coimbra – Portugal,* [7]*IRIBHM; Université Libre de Bruxelles, Brussels B-1070,* [8]*Division of Molecular Neurobiology, Department of Medical Biochemistry and Biophysics, Karolinska Institutet, S-17177 Stockholm, Sweden,* [9]*School of Medical Sciences, University of Aberdeen, Aberdeen AB25 2ZD, United Kingdom,* [10]*Team Dynamic and Pathophysiology of Neuronal Networks, Center for Interdisciplinary Research in Biology, College de France, CNRS UMR7241/INSERM U1050, Paris, France,*

1

Correspondence: Dr A Köfalvi, Laboratory of Neuromodulation and Metabolism, Center for Neuroscience and Cell Biology, Faculty of Medicine, University of Coimbra, 3004-504 Coimbra, Portugal. Tel: +3512 3982 0190/ 126, E-mail: akofalvi@uc.pt

BACKGROUND AND PURPOSE: Both CB_1 cannabinoid and A_{2A} adenosine receptors (CB_1Rs and $A_{2A}Rs$) control synaptic transmission at corticostriatal synapses, with great therapeutic importance for neurological and psychiatric disorders. A post-synaptic CB_1R-$A_{2A}R$ interaction has already been unraveled, but the presynaptic $A_{2A}R$-mediated control of presynaptic neuromodulation by CB_1Rs remains to be defined. Since the corticostriatal terminals provide the major input of the basal ganglia, understanding the interactive nature of converging neuromodulation on them will provide us with novel powerful tools to understand the physiology of corticostriatal synaptic transmission and interpret changes associated with pathological conditions.

EXPERIMENTAL APPROACH: Here we employ selective presynaptic tools to study the putative presynaptic interaction between the two neuromodulator systems. Pharmacological manipulation of CB_1R and $A_{2A}R$ was carried out in isolated nerve terminals used for flow synaptometry, immunoprecipitation, radioligand binding, ATP and glutamate release measurement, as well as in whole-cell patch-clamp recordings in horizontal corticostriatal slices.

RESULTS: Flow synaptometry showed that $A_{2A}R$ are extensively co-localized with CB_1R-immunopositive corticostriatal terminals, and $A_{2A}R$ co-immunoprecipitated CB_1R in these purified terminals. $A_{2A}R$ activation decreased CB_1R radioligand binding and decreased the CB_1R-mediated inhibition of high-K^+-evoked glutamate release in corticostriatal terminals. Accordingly,

$A_{2A}R$ activation prevented CB_1R-mediated paired-pulse facilitation and attenuated the CB_1R-mediated inhibition of synaptic transmission in glutamatergic synapses of corticostriatal slices.

CONCLUSIONS AND IMPLICATIONS: These results show that presynaptic $A_{2A}R$ dampens CB_1R-mediated inhibition of corticostriatal terminals. This constitutes a thus far unrecognized mechanism to shut-down the potent CB_1R-mediated presynaptic inhibition, enabling a frequency-dependent enhancement of synaptic efficacy at corticostriatal synapses.

Abbreviations

3Rs, Replacement, Refinement and Reduction of Animals in Research; $A_1R(s)$, A_1 adenosine receptors; $A_{2A}R(s)$, A_{2A} adenosine receptor(s); ADA, adenosine deaminase; ARRIVE, Animals in Research: Reporting *In Vivo* Experiments; ATP, adenosine triphosphate; BDNF, brain-derived neurotrophic factor; $CB_1R(s)$, CB_1 cannabinoid receptor(s); CCD, charge-coupled device; DMSO, dimethylsulfoxide; EDTA, ethylenediaminetetraacetic acid; EPSC(s), excitatory post-synaptic potential(s); FACS, fluorescence-activated cell sorting; FELASA, Federation for Laboratory Animal Science Associations; FGF, fibroblast growth factor; FR%, fractional release percent; [^{3}H]GABA, tritiated γ-aminobutiric acid; GDNF, glial cell-derived neurotrophic factor; GTP, guanosine triphosphate; HEPES, 4-(2-hydroxyethyl)-1-piperazineethanesulfonic acid; IgG_{2A}, immunoglobulin G_{2A}; L-DOPA, L-3,4-dihydroxyphenylalanine; MSN(s), medium spiny neuron(s); OFA, Oncins France Strain A; PBS, phosphate-buffered saline; PPR, paired-pulse ratio; SDS, sodium dodecyl-sulphate; SDS-PAGE, sodium dodecyl sulfate/polyacrylamide gel electrophoresis; Tris, tris(hydroxymethyl)aminomethane; Triton-X 100, polyethylene glycol p-(1,1,3,3-tetramethylbutyl)-phenyl ether; vGlut1, vesicular glutamate transporter 1;

INTRODUCTION

The corticostriatal pathway is a massive projection linking virtually the entire neocortex with the striatum – the latter being considered as the major input station of the basal ganglia (Goldman-Rakic and Selemon, 1986; Bolam et al., 2000). The principal neurons of the striatum – medium spiny neurons (MSNs) – integrate synaptic information from functionally diverse cortical regions, to process signals controlling goal-directed behaviors and habits (Graybiel et al., 1995; Yin and Knowlton, 2006). As a gateway to trigger the recruitment of striatal circuits, alterations in the strength of the synaptic connections between the cortex and striatum play a critical role in these adaptive behavioral changes (Di Filippo et al., 2009).

G protein-coupled receptors such as the CB_1 cannabinoid receptor (CB_1R) are key determinants of synaptic efficacy changes in cortico-striatal synapses (Lovinger, 2010). Accordingly, the manipulation of the endocannabinoid system has a profound impact on striatal-dependent behavioral responses (El Manira and Kyriakatos, 2010; Katona and Freund 2012). Another major controller of striatal function is the A_{2A} adenosine receptor ($A_{2A}R$) (Schiffmann et al., 2007). These $A_{2A}Rs$ are abundantly located in the dendritic spines of MSNs (Svenningsson et al., 1999) and are also present presynaptically, controlling glutamate release (Ciruela et al., 2006; Quiroz et al., 2009) and cortico-striatal plasticity (D'Alcantara et al., 2001; Flajolet et al., 2008). Interestingly, $A_{2A}Rs$ seem to mainly act as a fine-tuning system, adapting the efficiency of different other modulator systems (Sebastião and Ribeiro, 2000; Ferré et al., 2011). The activation of striatal $A_{2A}Rs$ results in G_s-mediated accumulation of cAMP (G_{olf} in the MSNs), in contrast to the stimulation of the other abundant striatal adenosine receptor, the inhibitory $G_{i/o}$-coupled A_1 adenosine receptors (A_1Rs, Dunwiddie and Masino, 2001). In physiological conditions, low-frequency ($0.1 <$ Hz) neuronal activity is accompanied with a modest generation

of adenosine, likely from the metabolism of ATP of astrocytic origin, which exerts tonic inhibition of neighbouring excitatory synapses via A_1Rs (Cunha, 2008). This dominant form of paracrine adenosinergic neuromodulation probably serves as to decrease the noise of the system at resting state (Cunha, 2008). In contrast, under high-frequency discharge of the nerve terminals, the ecto-5'-nucleotidase-mediated degradation of ATP, co-released from synaptic vesicles (Sperlágh and Vizi, 1996), will build up synaptic adenosine levels that are sufficient for autocrine A_{2A}R activation (Cunha, 2008; Augusto et al., 2013). Pathological conditions such as ischemia can also increase extracellular adenosine levels via outward transport, which are enough to stimulate both A_1Rs and A_{2A}Rs (Gomes et al., 2011).

A_{2A}R have been reported to tightly regulate the endocannabinoid neuromodulation system in the striatum, as heralded by the documented A_{2A}R-CB_1R interactions in the control of motor dysfunction (Ferré et al., 2010; Lerner et al., 2010; Tozzi et al., 2012) and addiction (Soria et al., 2004; Yao et al., 2006; Rosi et al., 2010; Justinová et al., 2011). This is re-enforced by the reported heteromerization of A_{2A}R with CB_1R that was demonstrated in heterologous expression systems and in the striatum (Carriba et al., 2007). However, this A_{2A}R-CB_1R interaction is mostly interpreted as resulting from a postsynaptic interaction (Yao et al., 2006; Rossi et al., 2010; Cerri et al., 2014; Pinna et al., 2014), whereas the predominant localization of CB_1R is presynaptic in the striatum (Köfalvi et al., 2005; Uchigashima et al., 2007). A possible presynaptic interaction between A_{2A}R and CB_1R has also been proposed to control the motor-depressant and addictive effects of cannabinoids (Ferré et al., 2010; Martire et al., 2011; Justinová et al., 2014), yet detailed experimental evidence is lacking. Here we set our aims to further expand our previous observations (Matíre et a., 2011) now with selective presynaptic techniques, combining refined immunological, radioligand binding and functional assays to directly investigate A_{2A}R-CB_1R interaction in glutamatergic nerve terminals of cortico-striatal synapses.

5

METHODS

Subjects

All studies were conducted in accordance with the principles and procedures outlined as "3Rs" in the guidelines of EU (86/609/EEC), FELASA, and the National Centre for the 3Rs (the ARRIVE; Kilkenny et al., 2010), and were approved by the Animal Care Committee of the Center for Neuroscience and Cell Biology of Coimbra and by the Centre for Interdisciplinary Research in Biology in College de France.

Animals were housed with 12 h light on/off cycles and *ad libitum* access to food and water. Forty-nine male Wistar rats (180-240 g, 8-10-week old) were purchased from Charles-River (Barcelona, Spain) and 6 OFA (Oncins France Strain A) rats (16-22 post-natal days) from Charles–River (L'Arbresle, France). Five pairs of $A_{2A}R$ and CB_1R null-mutant (knockout) male mice on CD-1 background (Ledent et al., 1997, 1999) and their wild-type littermates (35-45 g, 8-12-week old) were also used and were genotyped by tail snips.

Synaptosomal preparations

Experimental procedures were carried out as previously described (Ferreira et al., 2009). Briefly, the animals were decapitated under halothane anesthesia, and their brains were quickly removed into ice-cold 0.32 M sucrose solution containing 5 mM HEPES, 1 mM EDTA, and 1/500 v/v protease inhibitor cocktail Sigma-Aldrich (Saint Louis, MO, USA), pH 7.4, homogenized instantly and centrifuged at 3,000 *g* for 5 min. The supernatant was collected and centrifuged at 13,000 *g* for 10 min to obtain the P2 crude synaptosomal fraction. For immunolabeling and flow cytometry analysis, the P2 fraction was further purified in

discontinuous Percoll gradient (3, 10 and 23%), as described in Köfalvi et al. (2005). The purified synaptosomes were kept at -80 ℃ until use.

Immunolabeling and flow cytometric analysis of purified nerve terminals

Immunochemical labeling was performed according to a method for staining of intracellular antigens (Schmid et al., 1991; Gylys et al., 2000), with little modification. Briefly, purified nerve terminals were fixed in 1 mL of 0.25% paraformaldehyde in phosphate-buffered saline (PBS: 135 mM NaCl, 1.3 mM KCl, 3.2 mM NaH_2PO_4 and 0.5 mM KH_2PO_4) for 1 hour at 4 ℃ and then centrifuged at 3000 g for 3 min at 4 ℃. For permeabilization, the pellets were incubated in PBS with 0.2% Tween-20 for 15 min at 37 ℃ and then centrifuged at 3000 g for 3 min. The pellets were then resuspended in PBS for immunolabeling. Primary and secondary antibodies (Supporting Information Table S1) were diluted in PBS containing 2% normal goat serum (Vector Laboratories, CA, USA). For validation/titration of the primary antibodies see Supporting Information Figure S1. Incubation volume was 100 uL and incubation time was 30 min at 4 ℃ for both the primary and the secondary antibodies. Each incubation was followed by 3 times washing in PBS with 0.2% tween-20 and centrifugation at 3000 g for 3 min. The samples were resuspended in filtered PBS for flow-synaptometric analysis.

Analysis was performed using a FACSCalibur flow cytometer (Becton, Dickinson and Company, USA – equipped with a 488 nm argon-ion laser). Sample flow was set at 350 events per second; 50,000 ungated events were collected for analysis. A threshold was set on forward light scatter to exclude debris. To correct for spectral overlap during multicolor flow cytometry experiments, color compensation was performed. Offline data analysis was performed using BD Cell Quest Pro software (Becton, Dickinson and Company, USA). For detailed description see Supporting Information Figure S1.

Receptor binding

Synaptosomal membranes were prepared as previously described (Rebola et al., 2005) upon resuspensions of P2 synaptosomes in 2 mL of ice-cold assay solution [50 mM Tris/HCl, 3 mM MgCl$_2$, 1 µM CaCl$_2$, 2 mM EDTA and protease inhibitor cocktail (Sigma), pH 7.4]. Single point CB$_1$R binding experiment with 3.82±0.29 nM (n=7) of the CB$_1$R antagonist/inverse agonist, [^{3}H]SR141716A was carried out as before (Ferreira et al., 2012), with 30 min preincubation in the presence of adenosine deaminase (ADA, 2 U/mL) and of the diacylglycerol lipase inhibitor, OMDM188 (300 nM, a kind gift of Dr. Vincenzo Di Marzo). Non-specific binding was determined by using the CB$_1$R antagonist/inverse agonist, AM251 (1 µM). Each of the 7 independent assays were carried out on synaptic membranes derived from 2 rats, altogether 14 rats, and assayed in quadruplicate (28 filters/ condition). The tritium content of each sample was counted using a Tricarb 2900TR β-counter (PerkinElmer). The specific binding was expressed as amount of ligand specifically bound per milligram of protein.

Immunoprecipitation

Immunoprecipitation assays were carried out in both crude and Percoll-purified rat striatal synaptosomal fractions (pooled from 3 rats to obtain enough material), as previously described (Marques et al., 2013). Briefly, protein extracts were incubated with 50% protein G-sepharose bead slurry (GE Healthacare, UK) for 3 hours at 4 ºC to eliminate non-specific binding. After incubation, the precleared supernatants containing 1 mg protein were incubated overnight with rotation at 4 °C with a mouse anti-A$_{2A}$R antiserum (Millipore) pre-coupled covalently to protein G-sepharose (GE Healthacare), in the presence of 1% bovine serum albumin (Sigma) and protease inhibitors (Roche Diagnostics). The beads were washed 3 times with isolation buffer containing 150 mM KCl, 20 mM 3-(N-morpholino)propanesulfonic acid and 1% Triton X-100

(pH 7.4) and resuspended in 6× diluted SDS-PAGE sample buffer (0.35 M Tris, 30% glycerol, 10% SDS, 0.6 M dithiothreitol, 0.012% bromophenol blue [pH 6.8]). Bound proteins eluted from the immune complexes were denatured by heating to 95ºC for 5 min and then separated by electrophoresis on SDS-PAGE gels. Proteins were then electrotransferred onto nitrocellulose membranes (Amersham) and probed with rabbit anti-CB_1R (Table S1) and mouse anti-$A_{2A}R$ (Table S1) diluted in Tris-buffered saline supplemented with Tween 20 (0.1% v/v) and bovine serumalbumine (5% m/v). Immunoreactivity was visualized using horseradish peroxidase-conjugated goat anti-rabbit or anti-mouse secondary antibodies (Pierce) with a subsequent incubation with SuperSignal West Pico Chemiluminescent Substrate (Pierce), and the images were acquired using Versadoc3000 apparatus and analysed with ImageLab software (BioRad). A negative control containing the same amount of mouse IgG_{2A} instead of the mouse anti-$A_{2A}R$ antibody was run in parallel for each experiment.

[^{14}C]glutamate release

Experiments were carried out with slight modifications to previous publications (Köfalvi et al., 2005), which are: the synaptosomes were loaded with [^{14}C]-U-glutamate (20 µM) for 10 min, and the superfused synaptosomes, trapped in the 16-microvolume chamber release system, were stimulated with 30 mM KCl twice fir 1 min (S_1, S_2), with a 10-min interval. All Krebs-HEPES solutions used for this assay contained the habitual glutamate decarboxylase inhibitor aminooxy acetic acid (100 µM) to prevent [^{14}C]glutamate degradation. For detailed discription, see Köfalvi et al. (2005) and Ferreira et al. (2009). The validation of the A_1R, $A_{2A}R$ as well as CB_1R-mediated neuromodulation in Wistar rat and CD-1 mouse striatal synaptosomes is summarized in Table S2.

ATP release assay from striatal synaptosomes

ATP quantification was carried out in 96-well plates, by the help of a Perkin Elmer Victor[3] multilabel plate reader in luminometer mode. The ATP assay mix (Sigma-Aldrich) used by us allows quantitative bioluminescent determination of very low ATP levels ranging from 2×10^{-12} to 8×10^{-5} M, according to Navizet et al. (2011). Solutions used: i) Basal saline medium (in mM): 115 NaCl, 3 KCl, 1.2 KH_2PO_4, 25 HEPES, 10 glucose, 1.2 $MgSO_4$, 1 $CaCl_2$, pH = 7.4; and ii) potassium saline medium (in mM): 118 KCl, 1.2 KH_2PO_4, 25 HEPES, 10 glucose, 1.2 $MgSO_4$, 1 $CaCl_2$, pH = 7.4. A 150 μL aliquot of basal saline medium (+treatment/vehicle), 15 μL of ATP assay mix and 35 μL synaptosomal suspension (~1 mg/mL) provided the 200 μL final reaction volume. This mixture was incubated at 25 ℃ during 3 min in an Eppendorf tube to ensure functional recovery of the sample, then was transferred into a well of the plate at 25 ℃, inside the reader. Afterwards, a kinetic protocol was initiated with the duration 140 sec. During first 60 sec, a stable baseline was recorded corresponding to the basal extrasynaptic ATP level. Subsequently, synaptosomes were stimulated with KCl (30 mM) or were challenged only with the same amount of NaCl serving as osmotic control. Average readings in the presence of high NaCl were subtracted from KCl-stimulated average readings.

Electrophysiology

Whole-cell patch-clamp recordings from medium spiny neurons were performed in horizontal brain slices from OFA rats (Figure 5A) (postnatal days 15–22), as previously described (Fino et al. 2005). Briefly, the artificial cerebrospinal fluid (containing in (mM): 125 NaCl, 2.5 KCl, 25 glucose, 25 $NaHCO_3$, 1.25 NaH_2PO_4, 2 $CaCl_2$, 1 $MgCl_2$, and 10 μM pyruvic acid bubbled with 95% O_2 and 5% CO_2); the borosilicate glass pipettes (6-8 MΩ) contained (in mM):

105 potassium gluconate, 30 KCl, 10 HEPES, 10 phosphocreatine, 4 ATP-Mg, 0.3 GTP-Na, 0.3 EGTA (adjusted to pH 7.35 with KOH). All the experiments were carried in the presence of 50 μM picrotoxin (Sigma-Aldrich). Electrical stimulation was performed with a bipolar electrode (Phymep, Paris, France), placed at the layer 5 of the somatosensory cerebral cortex, by applying a monophasic and constant current (duration: 100–150 μs) (ISO-Flex stimulator controlled by a Master-8, A.M.P.I., Jerusalem, Israel). All recordings were performed at 32 ℃ using a temperature control system (Bath-controller V, Luigs & Neumann, Ratingen, Germany). Individual neurons were identified using infrared differential interference contrast microscopy with CCD camera (Hamamatsu C2400-07; Hamamatsu, Japan). Signals were amplified using an EPC9-2 amplifier (HEKA Elektronik, Lambrecht, Germany). The range of access resistance was 80–200 MΩ. The liquid junction potential was calculated and corrected. Voltage-clamp recordings were filtered at 5 kHz and sampled at 10 kHz using he program Pulse-8.53 (HEKA Elektronik). The series resistance was compensated at 75-80 % and variation of series resistance above 20% led to the rejection of the experiment. Off-line analysis was performed using Igor-Pro 6.0.3 (Wavemetrics, Lake Oswego, OR, USA).

Data treatment

Raw effect data from [^{14}C]glutamate and ATP release assays and from electrophysiology were normalized to the appropriate control of the same experiment. These normalized data were tested for normality by the Kolmogorov-Smirnov normality test. Statistical significance was calculated by one-sample *t*-test against the hypothetical value of 100 (as 100%, *i.e.* vehicle control). Pairs of treatment or condition groups were compared with Student's paired *t*-test, while the antibody titration curves were compared with Two-way ANOVA between the WT and the KO mice. A $P < 0.05$ was accepted as significant difference.

Chemicals

1-(2,4-dichlorophenyl)-5-(4-iodophenyl)-4-methyl-N-(1-piperidyl)pyrazole-3-carboxamide (AM251), (R)-(+)-[2,3-dihydro-5-methyl-3-(4-morpholinylmethyl)pyrrolo[1,2,3-de]-1,4-benzoxazin-6-yl]-1-napthalenylmethanone (WIN55212-2) and (6aR,10aR)-6a,7,10,10a-tetrahydro-3-[5-(1H-imidazol-1-yl)-1,1-dimethylpentyl]-6,6,9-trimethyl-6H-dibenzo[b,d]pyran-1-ol (O-2545) were purchased from Abcam Biochemicals, UK; 3-[4-[2-[[6-amino-9-[(2R,3R,4S,5S)-5-(ethylcarbamoyl)-3,4-dihydroxy-oxolan-2-yl]purin-2-yl]amino]ethyl]phenyl]-propanoic acid (CGS21680) was purchased from Tocris Bioscience, UK; dimethylsulfoxide (DMSO), 3-(N-morpholino)propanesulfonic acid (MOPS), aminooxyacetic acid, halothane, HEPES, Percoll, adenosine deaminase (ADA), bovine serumalbumine, and sucrose were purchased from Sigma (Saint Louis, MO, USA). [^{3}H]SR141716A and [^{14}C]-U-glutamate were purchased from American Radiolabeled Chemicals (Saint Louis, MO, USA). All other reagents were purchased from MerckBiosciences (Darmstadt, Germany).

RESULTS

$A_{2A}R$ and CB_1R colocalize in corticostriatal glutamatergic nerve terminals

A basic first evidence to probe the functional cross-talk between CB_1R and $A_{2A}R$ in corticostriatal glutamatergic terminals is to demonstrate their simultaneous co-localization at these sites. Thus, we analyzed striatal synaptosomes via flow synaptometry (Figure 1A): we double-labeled them for synaptophysin and vesicular glutamate transporter type 1 (vGluT1) (Figure 1B), or triple-labeled for vGluT1, CB_1R and $A_{2A}R$ (Figure 1C-E). Concerning the double labeling, $85.2\pm2.5\%$ (n=3) of the analyzed particles were positive for synaptophysin. Of these particles, $58.5\pm3.5\%$ were positive for vGluT1 (Figure 1B). Triple labeling allowed to precisely

quantify that 49.4±3.3% of the vGluT1-positive terminals were endowed with CB_1R (n=3) (Figure 1C) and 30.9±1.7% beared $A_{2A}R$ (n=3) (Figure 1D). Additionally, 47.1±2.7% of the CB_1R-positive terminals were also positive for $A_{2A}R$ (n=3) (Figure 1E). In other words, as supported by Figure 1E, 75.1±3.6% (n=3) of $A_{2A}R+$ terminals are also positive for CB_1R in vGlut1+ nerve terminals.

Interestingly, the selectivity analysis of the CB_1R (Figure 2A) and the $A_{2A}R$ (Figure 2B) antibodies in the CB_1R and $A_{2A}R$ KO mice and their wild-type littermates (Supporting Information Figure S1) suggested that CB_1Rs help the targeting of $A_{2A}R$ to the presynapse: in fact, the titration (saturation binding) curve of the anti-$A_{2A}R$ antibody revealed a decrease of the number of binding sites in vGluT1-positive terminals of CB_1R KO compared to WT mice (n=5; $P<0.05$; Figure 2C), which was not accompanied by any change in antibody affinities to its respective receptor (Figure 2D)**.**

$A_{2A}R$ co-immunoprecipitates the CB_1R in striatal nerve terminals

The extensive co-localization of CB_1R-$A_{2A}R$ in nerve terminals hints at a possible physical interaction of $A_{2A}R$ and CB_1R, as reported in culture cells and striatal homogenates (Carriba et al., 2007). To test this hypothesis, we performed immunoprecipitation with an anti-$A_{2A}R$ antibody in both crude (the so-called P2 fraction) and in Percoll-purified striatal nerve terminals. Subsequent immunoblot analyses of the composition of the immunoprecipitates allowed detecting CB_1R at the expected ~51 kDa molecular weight, with particular enrichment in the $A_{2A}R$-immunoprecipitated fractions when compared to the initial (non-immunoprecipitated) homogenate (Figure 3).

The strong co-localization and co-immunoprecipitation data prompted us to test if $A_{2A}R$ activation affected CB_1R binding. Experiments were carried out under the minimization of

endogenous adenosine and 2-arachidonoyl-glycerol levels with ADA and OMDM188 (see Materials and Methods). A single point receptor binding assay showed that CGS21680 (30 nM) decreased the binding of the radiolabeled CB_1R-selective ligand, [^{3}H]SR141716A to synaptosomal membranes from 3.23 ± 0.17 to 2.68 ± 0.18 pmol/mg of protein (n=7 in quadruplicates, $P<0.05$) (figure not shown).

$A_{2A}R$ activation decreases the potency of CB_1R agonists in striatal glutamatergic terminals

Repetitive (S_1 and S_2) stimulation with high K^+ (30 mM for 1 min) triggered the release of similar amounts of [^{14}C]glutamate (Figure 4A) in a Ca^{2+}-dependent manner: the first stimulation-evoked release (S_1) was $54.1\pm5.8\%$ smaller in Ca^{2+}-free condition (10 mM $MgCl_2$ combined with 100 nM $CaCl_2$; n=6, $P<0.001$) when compared to that under normal condition. The CB_1R agonists, WIN55212-2 (0.1 - 3 μM; n≥6) or O-2545 (300 nM; n=5), added 4 min before the second stimulus (S_2), decreased the S_2/S_1 ratio (i.e. the second stimulus-evoked release) between $10.8\pm3.8\%$ to $45.4\pm4.5\%$, depending on the concentration used ($P<0.05$) (Figure 4A and 4B). The effect of WIN55212-2 was prevented by the selective CB_1R antagonist/inverse agonist AM251 (1 μM; n=6) present since the preperfusion period (Figure 4B). In contrast, neither the $A_{2A}R$ agonist, CGS21680 (30 nM) (Figure 4B) nor two $A_{2A}R$ antagonists had significant effect on the release of [^{14}C]glutamate evoked by either 15 or 30 mM K^+, and either in the rat or the CD-1 mouse striatal synaptosomes (see Table S2). This indicates that a possible occlusion of CGS21680 effect by either a too strong K^+ stimulus or by endogenous activation of $A_{2A}Rs$ was not the case.

However, CGS21680 when co-applied with WIN55212-2 (n≥6) or O-2545 (n=5), prevented the inhibition of the 30 mM K^+-evoked release of [^{14}C]glutamate by nanomolar concentrations of these CB_1R agonists (Figure 4B) ($P>0.05$ for CGS21680+WIN55212-2 [0.1

and 0.3 µM] vs. DMSO control). CGS21680 also significantly attenuated the inhibition by WIN55212-2 at 3 µM (n=6) (Figure 4B) (P<0.05 for CGS21680+WIN55212-2 [3 µM] vs. WIN55212-2 [3 µM] alone).

CB_1R activation attenuates ATP release in nerve terminals of the rat striatum

Although ATP is not only the source of adenosine, the endogenous agonist of the $A_{2A}Rs$, it is a co-transmitter to glutamate (Burnstock, 2013). In line with the above data on [^{14}C]glutamate release, we expected CB_1R activation to also suppress the release of ATP from striatal nerve terminals. Indeed, we observed that WIN55212-2 (1 µM) inhibited the high K^+-evoked release of ATP by $24.4_5 \pm 6.7\%$ (n = 6, $P < 0.05$) (Figure 4C and 4D), which was again prevented by the CB_1R antagonist, AM251 (1 µM), which *per se* did not alter the evoked release of ATP ($P > 0.05$) (Figure 4D).

$A_{2A}R$ activation inhibits CB_1R-mediated depression of glutamatergic transmission in the dorsolateral striatum

It is well known that CB_1R depress corticostriatal glutamatergic transmission (Gerdeman and Lovinger, 2001). Accordingly, the CB_1R agonist WIN55212-2 (500 nM) reduced the amplitude of evoked monosynaptic EPSCs by 17.5±5.0% after 5 min and by 37.9±12.5% after 16 min (n=8, $P<0.05$) (Figure 5B-D). The CB_1R antagonist AM251 (500 nM) prevented this WIN55212-2-induced depression of synaptic transmission while having no effect alone (n=5) (Figure 5D).

$A_{2A}R$ activation by CGS21680 (30 nM) also prevented the WIN55212-2-induced synaptic depression in the first 5 min (n=6, $P > 0.05$) but not at the later time-point, although the CB_1R-

15

mediated inhibition was smaller in the absence (-37.9±12.5%) than in the presence of CGS21680 (-29.7±6.1%, *P*<0.05) (Figure 5D). Of note, CGS21680 *per se* did not alter basal synaptic transmission (*P* > 0.05) (Figure 5D).

$A_{2A}R$ activation inhibits CB_1R-mediated increase in paired-pulse ratio

While changes in synaptic transmission can be a result of both pre- and post-synaptic events, an increase in the paired-pulse ratio (PPR) reflects presynaptic mechanisms (Schulz et al. 1994; Gerdeman and Lovinger, 2001). Thus, we analyzed the monosynaptic EPSC ratios of paired stimuli, delivered with a 25 ms interval (Figure 5A-C,E). The drug-naïve PPR mean value was 0.76±0.03 (n=22 cells from 6 rats) (Figure 5B and 5E). As shown in Figure 5C and E, 16 min application of WIN55212-2 (500 nM) led to a significant increase in PPR (by 34.6±17.9%, n=9, *P*<0.05), while a 5 min superfusion period with WIN55212-2 was still not enough to cause a significant PPR increase (by 6.4±4.7%, n=9, *P*>0.05). The CB_1R antagonist AM251 (500 nM) prevented the WIN55212-2-induced increase in PPR while having no effect alone (n=5) (Figure 5E).

In accordance with the previous findings, CGS21680 (30 nM, added 10 min before WIN55212-2) prevented WIN55212-2 from increasing the PPR (n≥6), while *per se* did not alter basal synaptic transmission (*P* > 0.05) (Figure 5E).

DISCUSSION

The present study provides direct evidence for the physical and functional interaction of $A_{2A}R$ and CB_1R in corticostriatal terminals. Indeed, we now provide for the first time direct evidence for the co-localization of both $A_{2A}R$ and CB_1R in the same, individually identified corticostriatal glutamatergic nerve terminal. It is important to note that the selectivity of

16

antibodies raises increasing concern in the scientific community (e.g. Grimsey et al., 2008). Here we carefully titrated our primary antibodies, and validated them in the knockout mice and their wild-type littermates whenever possible. This allowed us to avoid common mistakes, such as false co-localizations or misestimation of the frequency of labeling.

Furthermore, we showed that these A_{2A} and CB_1 receptors form presynaptic heteromers in purified striatal nerve terminals, which is a novel information, since this heterodimer was first identified in heterologous expression systems, and was reported to be also present in total striatal extracts (Carriba et al., 2007). Heterodimers can interact either at the level of intracellular signaling, or by modulating G protein availability, or simply by physically altering the conformation of the partner receptor (Franco et al., 2006; 2008). Our findings do not directly indicate the molecular nature of interaction, yet, we speculate from the binding data and the fact that the two receptors on their own utilize different pools of G proteins that the interaction involves physical modulation of conformation, rather that occurring at the level of G proteins.

This physical association of $A_{2A}R$ and CB_1R is suggestive of a tight functional interplay in the control of glutamatergic nerve terminals in the striatum. The functional consequences of this finding were revealed now with a combination of direct presynaptic tools of increasing complexity (radioligand binding in nerve terminal membranes, glutamate release assay in acutely isolated nerve terminals and paired-pulse ratio measurements in isolated monosynaptic contacts in corticostriatal slices), all of which showed that $A_{2A}R$ activation significantly attenuates CB_1R function. In particular, we documented the ability of $A_{2A}R$ to dampen the robust presynaptic CB_1R-mediated inhibition of corticostriatal glutamate release (Gerdeman and Lovinger, 2001; Köfalvi et al., 2005). This observation *per se* does not directly argue for a presynaptic location of the underlying $A_{2A}Rs$. However, as the CB_1Rs mediating the increase in the paired-pulse ratio are

presynaptic, we can indirectly infer that those $A_{2A}Rs$ co-localize presynaptically with these CB_1Rs, as also strongly suggested by the neurochemical data.

The physiological role of this presynaptic $A_{2A}R$-CB_1R complex is likely associated with the well-known high-pass filter phenomenon for corticostriatal activity (Bamford et al., 2004). In fact, it is well established that increased synaptic activity is directly coupled to an increased release of two of the most potent substances acting as presynaptic inhibitory feedback signals, namely the release of adenosine acting through inhibitory A_1Rs (Fredholm et al., 2005) and endocannabinoids acting through presynaptic CB_1Rs (Lovinger, 2010). The efficiency of these two presynaptic inhibitory system is best heralded by the observations that A_1Rs and CB_1Rs are highly abundant G protein-coupled receptors in the brain. During high-frequency discharge it is necessary to overcome these efficient presynaptic inhibitory systems to allow the passage of salient information. Therefore, high-pass filters become essencial to implement long-term increases of corticostriatal activity with relevant stimuli. The present results add a critical piece of evidence to suggest that $A_{2A}R$ participate in this high-pass filtering in response to phasic changes in synaptic adenosine levels (Cunha, 2008). Indeed, we and others have previously shown that ATP is co-released with glutamate (Pankratov et al., 2006) in a frequency-dependent manner (Wieraszko et al., 1989; Cunha et al., 1996). Furthermore, Augusto et al. (2013) have shown that adenosine, generated from ATP by ecto-5'-nucleotidase, constitutes the particular source that activates striatal $A_{2A}R$. In the case of a low frequency discharge, the corticostriatal terminals will not produce enough ATP-derived adenosine to activate presynaptic $A_{2A}R$ and the extracellular adenosine levels will be enough only to activate the inhibitory A_1R, as previously shown (Ciruela et al., 2006). Moreover, the glutamatergic activity will also produce retrograde inhibitory endocannabinoid signaling (Castillo et al., 2012; Katona and Freund, 2012). By contrast, salient and relevant information that should be encoded as increases of synaptic plasticity are associated

with a higher frequency of discharge of corticostriatal afferent; under such conditions, ATP-derived adenosine is now sufficient to activate $A_{2A}R$, which will play a double role of shunting down both presynaptic CB_1R inhibition, as now documented, as well as presynaptic A_1R inhibition (Ciruela et al., 2006). The engagement of $A_{2A}R$ has the additional potential of bolstering the function of different neurotrophins, such as BDNF (Sebastião and Ribeiro, 2009), GDNF (Gomes et al., 2009) as well as FGF (Flajolet et al., 2008), which further assist the implementation of long-term plastic changes in cortico-striatal synapses. Notably, $A_{2A}R$ are selectively engaged to control synaptic plasticity rather than basal synaptic transmission in different synapses (Rebola et al., 2008; Costenla et al., 2011), namely in corticostriatal synapses (D'Alcantara et al., 2001; Flajolet et al., 2008). This is in agreement with that CGS21680 failed to alter basal synaptic transmission under whole-cell patch-clamp configuration in the dorsolateral (somatosensory) striatum (present study) as well as in extracellular recording in the dorsomedial (associative) striatum (Martíre et al., 2011). Notably, Ciruela and colleagues (2006) reported a significant increase upon CGS21680 administration in the high-K^+-induced release of glutamate in striatal synaptosomes, which was not observed in the present study, in agreement with a previous study where 4-aminopyridine stimulation was used to provoke [^{14}C]glutamate release in striatal synaptosomes (Martíre et al., 2011), and with another report showing the lack of CGS21680 modulation on the high-K^+-induced release of [^{3}H]glutamate in hippocampal synaptosomes (Lopes et al., 2002). We can point out differences in the composition of the assay medium and in the execution of the experiments that may lead to the modification of CGS21680 effect in these assays.

This central hubbing role of $A_{2A}R$ as a high pass filter is likely to be further assisted by post-synaptic $A_{2A}R$, which inhibit D_2 dopamine receptor-mediated endocannabinoid production in the MSN dendrites (Lerner et al., 2010; Tozzi et al., 2012). Hence, adenosine will exert a

19

double lock onto endocannabinoid signaling to ensure the rescue of salient corticostriatal activity. Indeed, Bamford and colleagues (2004) noted that post-synaptic D_2R-mediated presynaptic inhibition of glutamate release is frequency-dependent, sparing only the most active corticostriatal terminals. This strongly corroborates our hypothesis.

Since the principal input, the "drive" of the whole basal ganglia is the corticostriatal pathway, the modulation of these afferents by presynaptic receptors will have profound effect on all basal ganglia-related lower- and higher-order brain functions including motor coordination, psychomotor drive, emotions, memory or decision making (Nakano et al., 2000). For instance, it is believed that the lack of D_2R-stimulated endocannabinoid synthesis in Parkinson's disease hampers presynaptic CB_1R-mediated control of corticostriatal afferents, leading to dyskinesias (Brotchie, 2003; Kreitzer and Malenka, 2007; Shen et al., 2008a). Additionally, we envisage an increased synaptic adenosine production and a further impairment of presynaptic CB_1R activity, even after L-DOPA administration. This could be one reason why $A_{2A}R$ blocking strategies are interesting as a palliative strategy adjunct to L-DOPA (Gomes et al., 2011). Another involvement of this newly described presynaptic heterodimer may be in drug addiction. It was recently found by some of these authors that the presynaptic $A_{2A}R$ facilitate the cocaine-induced psychomotor drive in corticostriatal terminals (Shen et al., 2008b, 2013), which once again can be explained by the negative control of $A_{2A}R$ on the CB_1R-mediated inhibition of these afferents.

Another example for the importance of this interaction implies that CB_1Rs exert neuroprotection both *in vitro* and *in vivo* in focal and global ichemia models (Nagayama et al., 1999; Melis et al., 2006). Hence, one can further speculate that ischemic activation of $A_{2A}Rs$ would hamper CB_1R-mediated neuroprotection. Indeed, $A_{2A}R$ blockade has been shown to be neuroprotective in several models (Gomes et al., 2011).

Altogether, the presynaptic $A_{2A}R$-CB_1R complex in corticostriatal terminals emerges as a novel module to optimize corticostriatal information processing. Additionally, the identification of this functional heteromer presynaptically, in the corticostriatal terminals, further strengthens the rationale of simultaneously targeting these two receptors rather than each individually, to achieve more efficient palliative therapies to alleviate striatal pathophysiology in motor and addictive diseases.

Acknowledgements

Conflicts of interest

None.

List of Author Contribution

Study design: AK, SGF, RAC. Flow synaptometry experiments: SGF, INC, TH. Co-IP: SGF, JMM, RJR. CB_1R binding assay: SGF, AK. Glutamate release experiments: SGF, AK. ATP measurement: FQG, ÂRT. Electrophysiology: SGF, LV. Source and genotyping of $A_{2A}R$ and CB_1R knockout mice and their wild-type littermates: CL. Financial support: AK, RAC, LV, TH. First draft: SGF.

REFERENCES

Alexander SP, Benson HE, Faccenda E, Pawson AJ, Sharman JL, Spedding M, et al. (2013). The Concise Guide to Pharmacology 2013/14: G Protein-Coupled Receptors. Br J Pharmacol. 170: 1459-1581.

Augusto E, Matos M, Sévigny J, El-Tayeb A, Bynoe MS, Müller CE, et al. (2013). Ecto-5'-nucleotidase (CD73)-mediated formation of adenosine is critical for the striatal adenosine A_{2A} receptor functions. J Neurosci 33: 11390-11399.

Bamford NS, Shang H, Schmitz Y, Wu NP, Cepeda C, Levine MS, et al. (2004). Heterosynaptic dopamine neurotransmission selects sets of corticostriatal terminals. Neuron 42: 653-663.

Bolam JP, Hanley JJ, Booth, PA, Bevan, MD (2000). Synaptic organization of the basal ganglia. J Anat 196: 527-542.

Brotchie JM (2003). CB_1 cannabinoid receptor signalling in Parkinson's disease. Curr Opin Pharmacol 3: 54-61.

Burnstock G (2013). Introduction to purinergic signalling in the brain. Adv Exp Med Biol 986: 1-12.

Carriba P, Ortiz O, Patkar K, Justinova Z, Stroik J, Themann A et al. (2007). Striatal adenosine A_{2A} and cannabinoid CB_1 receptors form functional heteromeric complexes that mediate the motor effects of cannabinoids. Neuropsychopharmacology 32: 2249-2259.

Castillo PE, Younts TJ, Chávez AE, Hashimotodani Y (2012). Endocannabinoid signaling and synaptic function. Neuron 76: 70-81.

Cerri S, Levandis G, Ambrosi G, Montepeloso E, Antoninetti GF, Franco R, et al. (2014) Neuroprotective potential of adenosine A_{2A} and cannabinoid CB_1 receptor antagonists in an animal model of Parkinson disease. J. Neuropathol. Exp Neurol 73: 414-424.

Ciruela F, Casadó V, Rodrigues RJ, Luján R, Burgueño J, Canals M, et al. (2006). Presynaptic control of striatal glutamatergic neurotransmission by adenosine A_1-A_{2A} receptor heteromers. J Neurosci 26: 2080-2087.

Costenla AR, Diógenes MJ, Canas PM, Rodrigues RJ, Nogueira C, Maroco J, Agostinho PM, Ribeiro JA, Cunha RA, de Mendonça A (2011). Enhanced role of adenosine A_{2A} receptors in the modulation of LTP in the rat hippocampus upon ageing. Eur J Neurosci 34: 12-21.

Cunha RA (2008). Different cellular sources and different roles of adenosine: A_1 receptor-mediated inhibition through astrocytic-driven volume transmission and synapse-restricted A_{2A} receptor-mediated facilitation of plasticity. Neurochem Int 52: 65-72.

Cunha RA, Vizi ES, Ribeiro JA, Sebastião AM (1996). Preferential release of ATP and its extracellular catabolism as a source of adenosine upon high- but not low-frequency stimulation of rat hippocampal slices. J Neurochem 67: 2180-2187.

d'Alcantara P, Ledent C, Swillens S, Schiffmann SN (2001). Inactivation of adenosine A_{2A} receptor impairs long term potentiation in the accumbens nucleus without altering basal synaptic transmission. Neuroscience 107: 455-464.

Di Filippo M, Picconi B, Tantucci M, Ghiglieri V, Bagetta V, Sgobio C, et al. (2009). Short-term and long-term plasticity at corticostriatal synapses: implications for learning and memory. Behav Brain Res 199: 108-118.

Dunwiddie TV, Masino SA (2001). The role and regulation of adenosine in the central nervous system. Annu Rev Neurosci 24: 31–55.

El Manira A, Kyriakatos A (2010). The role of endocannabinoid signaling in motor control. Physiology (Bethesda). 25: 230-238.

Ferré S, Lluís C, Justinová Z, Quiroz C, Orrú M, Navarro G et al. (2010). Adenosine-cannabinoid receptor interactions. Implications for striatal function. Br J Pharmacol 160: 443-453.

Ferré S, Quiroz C, Orru M, Guitart X, Navarro G, Cortès A et al. (2011). Adenosine A_{2A} receptors and A_{2A} receptor heteromers as key players in striatal function. Front Neuroanat 5: 1–8.

Ferreira SG, Lomaglio T, Avelino A, Oliveira CR, Cunha RA, Köfalvi A (2008). N-arachidonoyldopamine induces glutamate and dopamine release via a novel Ca^{2+} channel. Neuropharmacology 56: 676–683.

Ferreira SG, Teixeira FM, Garção P, Agostinho P, Ledent C, Cortes L, et al. (2012). Presynaptic CB_1 cannabinoid receptors control frontocortical serotonin and glutamate release – species differences. Neurochem Int 61: 219-226.

Fino, E, Glowinski J, Venance L (2005). Bidirectional activity-dependent plasticity at corticostriatal synapses. J Neurosci 25: 11279-11287.

Flajolet M, Wang Z, Futter M, Shen W, Nuangchamnong N, Bendor J, et al. (2008). FGF acts as a co-transmitter through adenosine A_{2A} receptor to regulate synaptic plasticity. Nature Neurosci 11: 1402-1409.

Franco R, Casadó V, Cortés A, Mallol J, Ciruela F, Ferré S, et al. (2008) G-protein-coupled receptor heteromers: function and ligand pharmacology. Br J Pharmacol 153:S 90-98.

Franco R, Casadó V, Mallol J, Ferrada C, Ferré S, Fuxe K, et al. (2006) The two-state dimer receptor model: a general model for receptor dimers. Mol Pharmacol 69: 1905-1912.

Fredholm BB, Chen JF, Cunha RA, Svenningsson P, Vaugeois JM (2005). Adenosine and brain function. Int Rev Neurobiol 63: 191-270.

Gerdeman GL, Lovinger DM (2001). Cannabinoid receptor inhibits synaptic release of glutamate in rat dorsolateral striatum. J Physiol 85: 468-471.

Goldman-Rakic PS and Selemon LD (1986). Topography of Corticostriatal Projections in Nonhuman Primates and Implications for Functional Parcellation of the Neostriatum. In Jones EG and Peters A (eds). Cerebral cortex. Plenum: New York, pp 447-466.

Gomes CA, Simões PF, Canas PM, Quiroz C, Sebastião AM, Ferré S, et al. (2009) GDNF control of the glutamatergic cortico-striatal pathway requires tonic activation of adenosine A receptors. J Neurochem 108: 1208-1219.

Gomes CV, Kaster MP, Tomé AR, Agostinho PM, Cunha RA (2011). Adenosine receptors and brain diseases: neuroprotection and neurodegeneration. Biochim Biophys Acta 1808: 1380-1399.

Graybiel AM (1995). Building action repertoires: memory and learning functions of the basal ganglia. Curr Opin Neurobiol 5: 733-741.

Grimsey NL, Goodfellow CE, Scotter EL, Dowie MJ, Glass M, Graham ES (2008). Specific detection of CB_1 receptors; cannabinoid CB_1 receptor antibodies are not all created equal! J Neurosci Methods 171: 78-86.

Gylys KH, Fein JA, Cole GM (2000). Quantitative characterization of crude synaptosomal fraction (P-2) components by flow cytometry. J Neurosci Res 61: 186-192.

Justinová Z, Ferré S, Redhi GH, Mascia P, Stroik J, Quarta D et al. (2011). Reinforcing and neurochemical effects of cannabinoid CB1 receptor agonists, but not cocaine, are altered by an adenosine A_{2A} receptor antagonist. Addict Biol 16: 405-415.

Justinová Z, Redhi GH, Goldberg SR, Ferré S (2014). Differential effects of presynaptic versus postsynaptic adenosine A_{2A} receptor blockade on Δ^9-tetrahydrocannabinol (THC) self-administration in squirrel monkeys. J Neurosci 34:6480-6484.

Katona I, Freund TF (2012). Multiple functions of endocannabinoid signaling in the brain. Annu Rev Neurosci 35: 529-558.

Kilkenny C, Browne W, Cuthill IC, Emerson M, Altman DG; NC3Rs Reporting Guidelines Working Group (2010). Animal research: reporting in vivo experiments: the ARRIVE guidelines. Br J Pharmacol 160: 1577-1579.

Köfalvi A, Rodrigues RJ, Ledent C, Mackie K, Vizi ES, Cunha RA, et al (2005). Involvement of cannabinoid receptors in the regulation of neurotransmitter release in the rodent striatum: a combined immunochemical and pharmacological analysis. J Neurosci 25: 2874-2884.

Kreitzer AC, Malenka RC (2007). Endocannabinoid-mediated rescue of striatal LTD and motor deficits in Parkinson's disease models. Nature 445: 643-647.

Ledent C, Vaugeois JM, Schiffmann SN, Pedrazzini T, El Yacoubi M, Vanderhaeghen JJ et al. (1997). Aggressiveness, hypoalgesia and high blood pressure in mice lacking the adenosine A_{2A} receptor. Nature 388: 674-678.

Ledent C, Valverde O, Cossu G, Petitet F, Aubert JF, Beslot F et al. (1999). Unresponsiveness to cannabinoids and reduced addictive effects of opiates in CB1 receptor knockout mice. Science 283: 401-404.

Lerner TN, Horne EA, Stella N, Kreitzer AC (2010). Endocannabinoid signalling mediates psychomotor activation by adenosine A_{2A} antagonists. J Neurosci 30: 2160-2164.

Lopes LV Cunha RA, Kull B, Fredholm BB, Ribeiro JA (2002). Adenosine A_{2A} receptor facilitation of hippocampal synaptic transmission is dependent on tonic A_1 receptor inhibition. Neuroscience. 112: 319-329.

Lovinger DM (2010). Neurotransmitter role in synaptic modulation, plasticity and learning in the dorsal striatum. Neuropharmacology 58: 951-961.

Martire A, Tebano MT, Chiodi V, Ferreira SG, Cunha RA, Köfalvi A, et al. (2011). Pre-synaptic adenosine A_{2A} receptors control cannabinoid CB_1 receptor-mediated inhibition of striatal glutamatergic neurotransmission. J Neurochem 116: 273-280.

Marques JM, Rodrigues RJ, Valbuena S, Rozas JL, Selak S, Marin P, et al. (2013). CRMP2 tethers kainate receptor activity to cytoskeleton dynamics during neuronal maturation. J Neurosci 33: 18298-18310.

Melis M, Pillolla G, Bisogno T, Minassi A, Petrosino S, Perra S, et al. (2006). Protective activation of the endocannabinoid system during ischemia in dopamine neurons. Neurobiol Dis 24: 15-27.

Nagayama T, Sinor AD, Simon RP, Chen J, Graham SH, Jin K, et al. (1999). Cannabinoids and neuroprotection in global and focal cerebral ischemia and in neuronal cultures. J Neurosci 19: 2987-2995.

Nakano K, Kayahara T, Tsutsumi T, Ushiro H (2000). Neural circuits and functional organization of the striatum. J Neurol 247: 1-15.

Navizet I, Liu YJ, Ferré N, Roca-Sanjuán D, Lindh R (2011) The chemistry of bioluminescence: an analysis of chemical functionalities. Chemphyschem 12: 3064-3076.

Pankratov Y, Lalo U, Verkhratsky A, North RA (2006) Vesicular release of ATP at central synapses. Pflugers Arch Eur J Physiol 452: 589-597.

Pinna A, Bonaventura J, Farré D, Sánchez M, Simola N, Mallol J, et al. (2014). L-DOPA disrupts adenosine A_{2A}-cannabinoid CB_1-dopamine D_2 receptor heteromer cross-talk in the striatum of hemiparkinsonian rats: biochemical and behavioral studies. Exp Neurol 253: 180-191.

Quiroz C, Luján R, Uchigashima M, Simoes AP, Lerner TN, Borycz J et al. (2009). Key modulatory role of presynaptic adenosine A_{2A} receptors in cortical neurotransmission to the striatal direct pathway. ScientificWorldJournal 9: 1321–1344.

Rebola N, Canas PM, Oliveira CR, Cunha RA (2005). Different synaptic and subsynaptic localization of adenosine A_{2A} receptors in the hippocampus and striatum of the rat. Neuroscience 132: 893-903.

Rebola N, Lujan R, Cunha RA, Mulle C (2008). Adenosine A_{2A} receptors are essential for long-term potentiation of NMDA-EPSCs at hippocampal mossy fiber synapses. Neuron 57: 121-134.

Rossi S, De Chiara V, Musella A, Mataluni G, Sacchetti L, Siracusano A, et al. (2010). Effects of caffeine on striatal neurotransmission: focus on cannabinoid CB_1 receptors. Mol Nutr Food Res 54: 525-531.

Schiffmann SN, Fisone G, Moresco R, Cunha RA, Ferré S (2007). Adenosine A_{2A} receptors and basal ganglia physiology. Prog Neurobiol 83: 277-292.

Schmid I, Uittenbogaart CH, Giorgi JV (1991). A gentle fixation and permeabilization method for combined cell surface and intracellular staining with improved precision in DNA quantification. Cytometry 12: 279-285.

Schulz PE, Cook EP, Johnston D (1994). Changes in paired-pulse facilitation suggest presynaptic involvement in long-term potentiation. J Neurosci 14: 5325-5337.

Sebastião AM, Ribeiro JA (2000). Fine-tuning neuromodulation by adenosine. Trends Pharmacol Sci 21: 341-346.

Sebastião AM, Ribeiro JA (2009). Triggering neurotrophic factor actions through adenosine A_{2A} receptor activation: implications for neuroprotection. Br J Pharmacol 158: 15-22.

Shen W, Flajolet M, Greengard P, Surmeier DJ (2008a). Dichotomous dopaminergic control of striatal synaptic plasticity. Science 321: 848-851.

Shen HY, Coelho JE, Ohtsuka N, Canas PM, Day YJ, Huang QY, et al. (2008b). A critical role of the adenosine A_{2A} receptor in extrastriatal neurons in modulating psychomotor activity as revealed by opposite phenotypes of striatum and forebrain A_{2A} receptor knock-outs. J Neurosci 28: 2970-2975.

Shen HY, Canas PM, Garcia-Sanz P, Lan JQ, Boison D, Moratalla R et al. (2013). Adenosine A_{2A} receptors in striatal glutamatergic terminals and GABAergic neurons oppositely modulate psychostimulant action and DARPP-32 phosphorylation. PLoS One 8: e80902.

Soria G, Castañé A, Berrendero F, Ledent C, Parmentier M, Maldonado R, et al. (2004). Adenosine A_{2A} receptors are involved in physical dependence and place conditioning induced by THC. Eur J Neurosci 20: 2203-2213.

Sperlágh B, Vizi ES (1996). Neuronal synthesis, storage and release of ATP. Semin Neurosci 8: 175–186.

Svenningsson P, Le Moine C, Fisone G, Fredholm BB (1999). Distribution, biochemistry and function of striatal adenosine A_{2A} receptors. Prog Neurobiol 59: 355-396.

Tozzi A, de Iure A, Marsili V, Romano R, Tantucci M, Di Filippo M et al. (2012). A_{2A} adenosine receptor antagonism enhances synaptic and motor effects of cocaine via CB_1 cannabinoid receptor activation. PLoS One 7: e38312.

Uchigashima M, Narushima M, Fukaya M, Katona I, Kano M, Watanabe M (2007). Subcellular arrangement of molecules for 2-arachidonoyl-glycerol-mediated retrograde signaling and its physiological contribution to synaptic modulation in the striatum. J Neurosci 27: 3663–3676.

Wieraszko A, Goldsmith G, Seyfried TN (1989). Stimulation-dependent release of adenosine triphosphate from hippocampal slices. Brain Res 485: 244-250.

Yao L, McFarland K, Fan P, Jiang Z, Ueda T, Diamond I (2006). Adenosine A_{2a} blockade prevents synergy between mu-opiate and cannabinoid CB_1 receptors and eliminates heroin-seeking behavior in addicted rats. Proc Natl Acad Sci U S A 103: 7877-7782.

Yin HH and Knowlton BJ (2006). The role of the basal ganglia in habit formation. Nature Rev Neurosci 7: 464-476.

Figure 1 Flow-synaptometric analysis of immunolabeled Percoll-gradient purified striatal synaptosomes. (A) Representative flow synaptometry plot of striatal synaptosomes for size (forward scatter is proportional to the particle diameter), and for complexity/granularity (side scatter). (B) Representative plot and statistics of synaptosomes double-labeled for synaptophysin (a marker of synaptosomes) and vesicular glutamate transporter 1 (vGluT1; a marker of corticostriatal terminals). (C and D) Representative plots and statistics of synaptosomes labeled for vGluT1/CB_1R (C) and vGluT1/$A_{2A}R$ (D), respectively (the two graphs are derived from the same triple-labelled sample). (E) Representative plot and statistics of vGluT1-positive synaptosomes expressing CB_1R and $A_{2A}R$. Note that most of the nerve terminals endowed with $A_{2A}Rs$ were also endowed with CB_1Rs.

Figure 2 (A) Total binding isotherms of the anti-CB_1R antibody in the corticostriatal terminals of the WT (squares) versus the $A_{2A}R$ KO mice (circles), while the CB_1R KO mice display antibody binding of non-specific nature only (triangles). (B) Total binding isotherms of the anti-$A_{2A}R$ antibody in the corticostriatal terminals of the WT (squares) versus the CB_1R KO mice (circles), while the $A_{2A}R$ KO mice display antibody binding of non-specific nature only (triangles). (C) Bar graphs representing the mean values of the maximum binding sites (B_{max}) of the anti-CB_1R and anti-$A_{2A}R$ antibodies (*$P<0.05$). (D) Bar graphs representing the mean changes of the dissociation constant (K_d) of the anti-CB_1R and anti-$A_{2A}R$ antibodies. Bars represent the mean ± SEM of 5 individual experiments.

Figure 3 Co-immunoprecipitation of A_{2A}Rs and CB_1Rs in crude (P2 fraction) and Percoll-purified striatal synaptosomes. CB_1R was readily detected and enriched in complexes immunoprecipitated with the anti-A_{2A}R, but not with mouse IgG_{2A}, either in P2 or or Percoll-purified fractions of rat striatal synaptosomes.

Figure 4 (A) Fractional release percent (FR%; see Methods) diagram representing the averaged [^{14}C]glutamate release curves in rat striatal synaptosomes under treatment with WIN55212-2 (1 μM; circles) and the respective control (triangles). Stimuli with high-K^+ (30 mM; 2×1 min) are marked as S_1 and S_2. WIN55212-2 was added as indicated by the horizontal line. Data are mean ± SEM of n = 21 independent observations in duplicate. (B) Bar graph representing the effect of the A_{2A}R activation on the CB_1R-induced inhibition of high-K^+-evoked release of [^{14}C]glutamate. The Y axis represents the effect of the treatment on the S_2/S_1 ratio, normalized to the vehicle control. WIN55212-2 *per se* (open bars) significantly inhibited the release of [^{14}C]glutamate in all concentrations (0.1, 0.3, 1 and 3 μM). The inhibitory effect of WIN55212-2 on the S_2/S_1 ratio was prevented by the CB_1R antagonist AM251 (1 μM, applied since the preperfusion period, i.e. before S_1). The selective A_{2A}R agonist CGS216880 (30 nM, co-applied with WIN55212-2), which *per se* had no effect on the high-K^+-evoked release of [^{14}C]glutamate, prevented the action of WIN55212-2 at 0.1 and 0.3 μM and significantly attenuated the action of WIN55212-2 at 3 μM. Similarly, O-2545 (0.3 μM), another CB_1R agonist, inhibited the release of [^{14}C]glutamate (brown bar), and CGS21680 (30 nM) prevented that action. All bars are mean ± SEM derived from n ≥ 6 animals. *$P < 0.05$; **$P < 0.01$; ***$P < 0.001$ vs. DMSO control (red dashed line), and $^{#}P < 0.05$ vs without CGS21680. (C) Representative diagram of high-K^+ (32 mM) -evoked release of ATP from striatal nerve terminals. Stimulus with KCl is marked as S_1. Consistent with ATP being co-released with

glutamate, activation of the CB_1Rs by WIN55212-2 (1 μM) also inhibits the KCl-evoked release of ATP. (D) As represented in the bar graphs, the CB_1R-mediated inhibition of ATP release (n = 6; *P<0.05) was prevented by the CB_1R antagonist, AM251 (1 μM), which *per se* had no effect.

Figure 5 CB_1R activation decreases basal synaptic transmission and increases paired-pulse ratio in rat corticostriatal afferents, which is attenuated / prevented by the $A_{2A}R$ agonist CGS21680 (30 nM). (A) The whole-cell patch clamp configuration in 15-22 day-old rats' horizontal corticostriatal slices, with stimulation in the layer V of the adjacent neocortex and recording in the dorsolateral striatum. (B, C) Representative paired-pulse traces (25 ms interpulse interval) in the presence of WIN55212-2 (500 nM), and its vehicle, DMSO. (D) Bar graphs representing the EPSC amplitude values normalized to the pretreatment period after 5 and 16 min of WIN55212-2 perfusion. WIN55212-2 decreased EPSC amplitude at both time points, in a fashion sensitive to AM251, which *per se* (open bar) had no effect. Ten min pretreatment with CGS21680 attenuated the CB_1R-mediated inhibition of EPSC amplitudes. CGS21680 did not produce effect on its own (open bars). All bars are mean ± SEM derived from n ≥ 6 animals. *P<0.05 vs. 100% (pretreatment CTRL). (E) Bar graphs representing the normalized paired-pulse ratio (PPR; the second response in relation to the first response) at 5 and 16 minutes after the beginning of WIN55212-2 perfusion. The WIN55212-2-induced increase (*P<0.05) in the paired-pulse ratio was prevented both by AM251 and CGS21680, which had no effect per se (open bars).
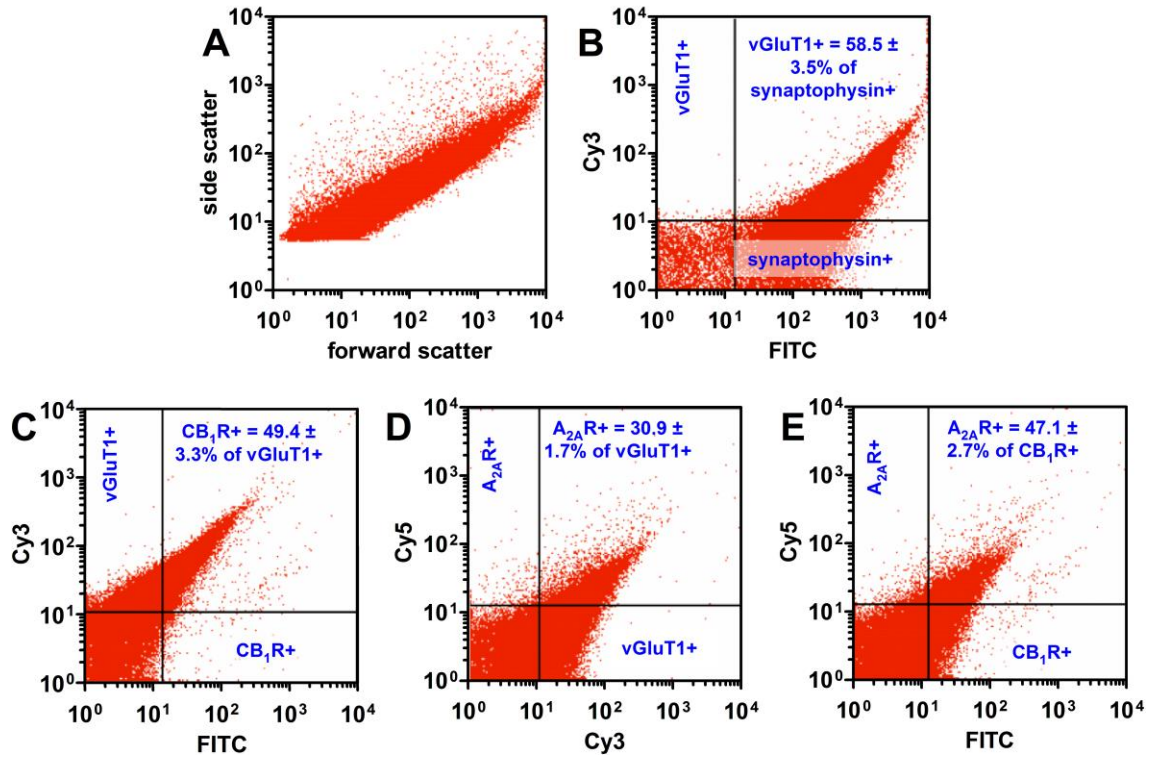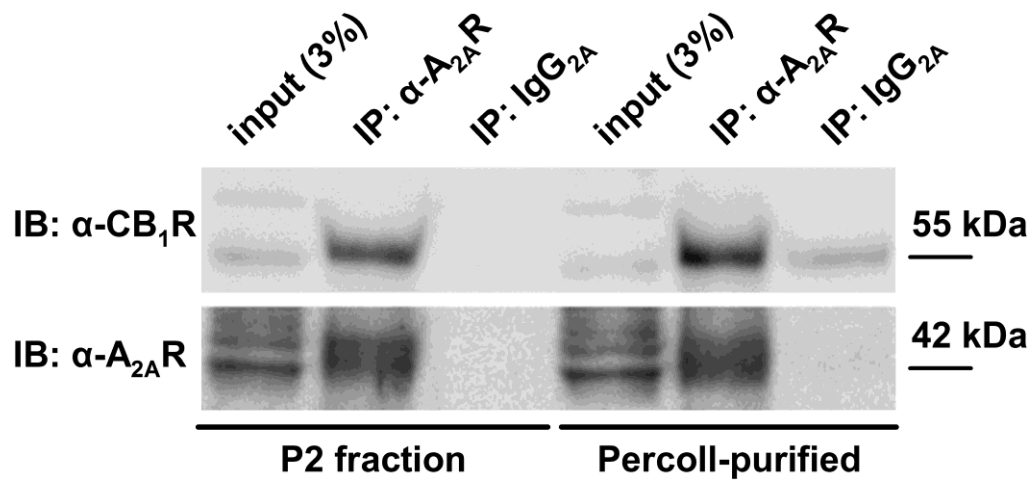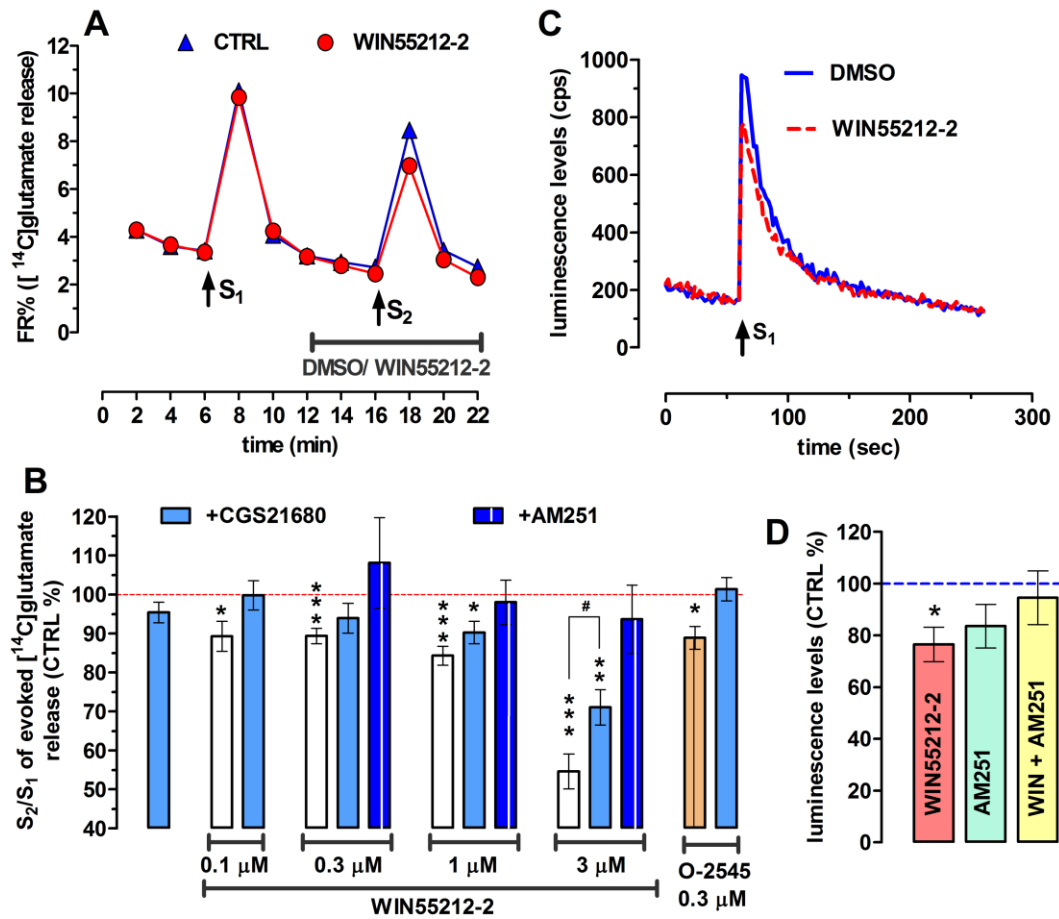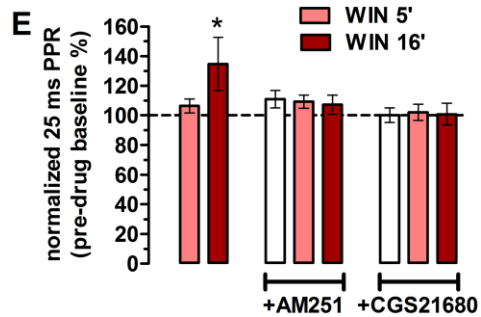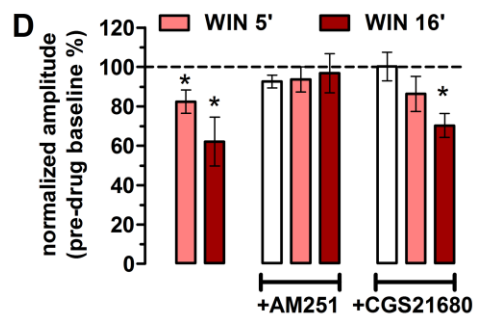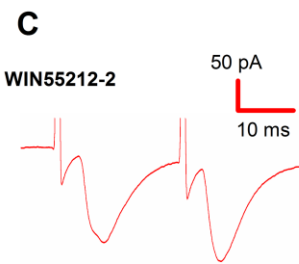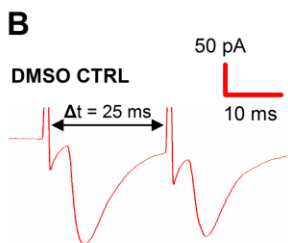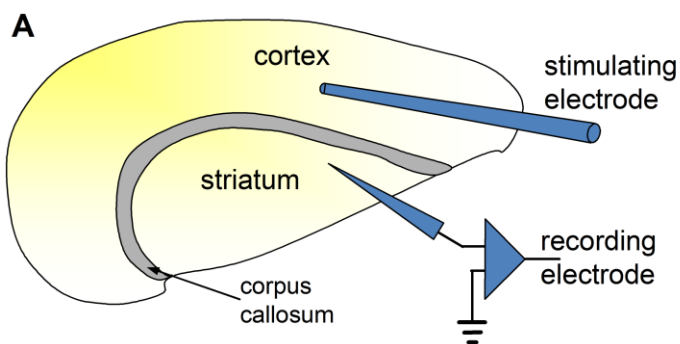
bph_12970_f1A-E
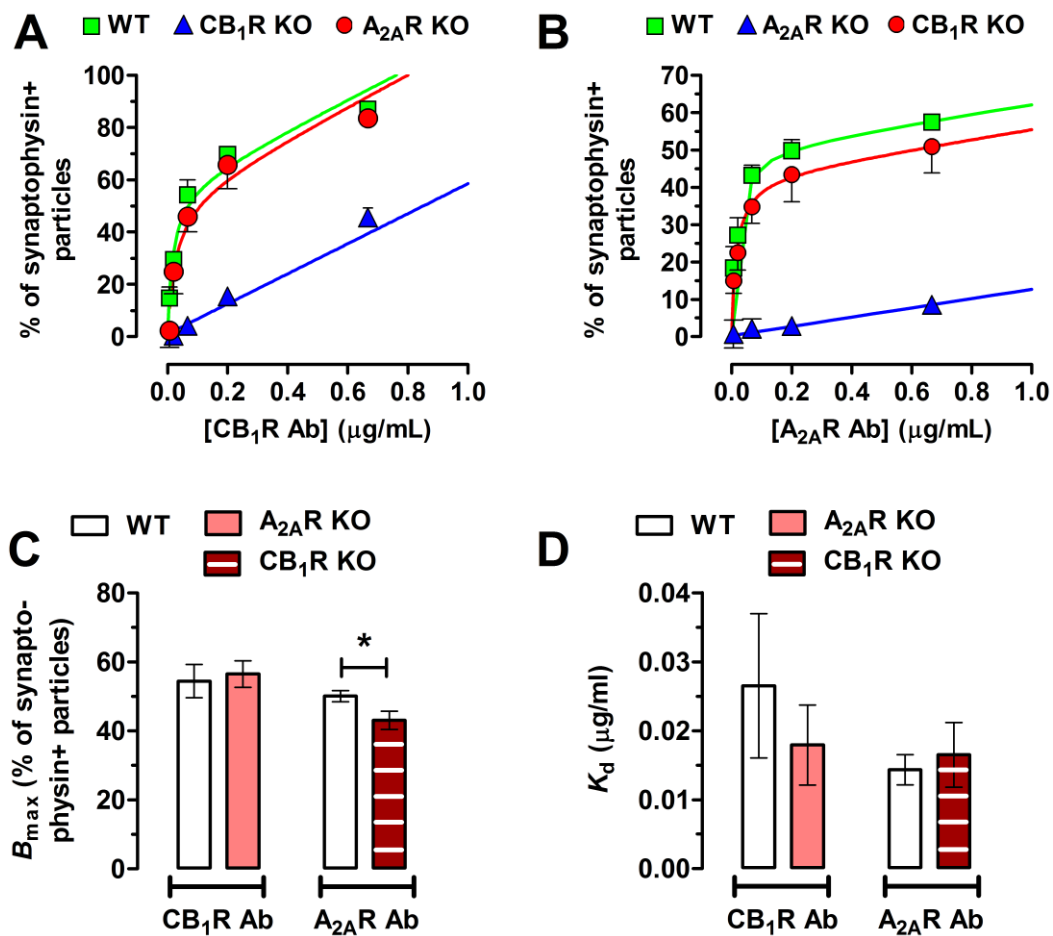
bph_12970_f2 A-D

bph_12970_f3

bph_12970_f4A-D

bph_12970_f5A-E